Crystal Structure, Spectroscopic, and Theoretical Investigations of Excited-State Proton Transfer in the Doubly Hydrogen-Bonded Dimer of 2-Butylamino-6-methyl-4-nitropyridine *N*-Oxide

Anna Szemik-Hojniak,*,† Irena Deperasińska,‡ Lucjan Jerzykiewicz,† Piotr Sobota,† Marek Hojniak,† Aniela Puszko,§ Natalia Haraszkiewicz,|| Gert van der Zwan,|| and Patrice Jacques^

Faculty of Chemistry, University of Wrocław, ul. Joliot-Curie 14, 50-383 Wrocław, Poland, Institute of Physics, Polish Academy of Sciences, Al. Lotników 32/46, 02-668 Warsaw, Poland, Institute of Chemical and Food Technology, University of Economics, Pl-53 345 Wrocław, Poland, Department of Analytical Chemistry and Applied Spectroscopy, Laser Centre, Vrije Universiteit, De Boelelaan 1083, 1081 HV Amsterdam, The Netherlands, and Department of Photochemistry, Université de Haute-Alsace, E. N. S. C. Mu, 3, rue Alfred Werner, F-68093 Mulhouse Cedex, France

Received: April 19, 2006; In Final Form: July 4, 2006

The crystal structure of 2-butylamino-6-methyl-4-nitropyridine *N*-oxide (2B6M) was resolved on the basis of X-ray diffraction. Solid 2B6M occurs in the form of a doubly hydrogen-bonded dimer with squarelike hydrogen-bonding network composed of two intra- (2.556(2) Å) and two intermolecular (2.891(2) Å) N−H···O type hydrogen bonds. The molecule thus has both a protonable and a deprotonable group that led us to investigate the possibility of an excited-state proton transfer (ESIPT) reaction in different solvents by means of experimental absorption, steady state, and time-resolved emission spectroscopy. The results were correlated with quantum mechanical TD-DFT and PM3 calculations. Experimental and theoretical findings show the possibility of an ESIPT reaction in polar solvents. It is demonstrated that in particular the emission spectra of 2B6M are very sensitive to solvent properties, and a large value of the Stokes shift (about 8000 cm^{-1}) in acetonitrile is indicative for an ESIPT process. This conclusion is further supported by time-resolved fluorescence decay measurents that show dual exponential decay in polar solvents. Vertical excitation energies calculated by TD-DFT reproduce the experimental absorption maxima in nonpolar solvents well. The majority of electronic transitions in 2B6M is of $\pi \rightarrow \pi^*$ character with a charge shift from the electron-donating to the electron-accepting groups. The calculations show that, due to the charge redistribution on excitation, the acidity of the amino group increases significantly, which facilitates the proton transfer from the amino to the *N*-oxide group in the excited state.

Introduction

Substituted pyridine *N*-oxides (Figure 1) form an interesting group of compounds that find use as catalysts,[1−4] reactive intermediates and drugs in pharmaceutical chemistry,[5−8] and ligands in metal complexes,[9] and they have been implicated as potentially useful in nonlinear optical devices.[10,11] The pyridine ring NO moiety can act as both an electron acceptor and an electron donor, of which the strength can be modulated by electron-donating or accepting-groups at other positions of the ring. Substitution of an *N*-alkyl group at the 2-position leads to the additional possibility of intra- and intermolecular proton transfer. Little is known about the photophysics of these compounds. Since some of them are biologically active,[12] an investigation of their optical properties and their possible use as probes for monitoring biochemical processes is useful.

Prototropic tautomerism in the molecular ground (GSIPT) and electronically excited states (ESIPT) has over the past 50 years attracted considerable attention. Since Weller's seminal work on the salicylic methyl ester,[13−15] a large body of experimental and theoretical work has been devoted to these reactions. In particular, salicylic acid derivatives[16−18] and hydroxyflavons[19−21] have been studied extensively for their possible use as probes for solvent properties, such as polarity and hydrogen-bonding capacity, and as probes for microenvironments (local electric fields) in proteins and membranes.[22] In addition, these reactions are challenging from a theoretical point of view.[23,24]

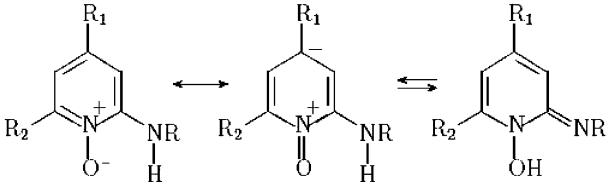

Figure 1. Substituted pyridine *N*-oxides. On the left, mesomeric forms of the normal (N) form. For the compound described in this article, R_1 is the nitro group NO_2, an electron-withdrawing group that favors the mesomeric structure in the middle. On the right, the proton transferred (PT) form, which no longer is aromatic.

Some of these compounds also allow the possibility of excited-state double proton transfer (ESDPT) reactions, in

* Corresponding author. E-mail: anias@wchuwr.chem.uni.wroc.pl.
† University of Wrocław.
‡ Polish Academy of Sciences.
§ University of Economics.
|| Vrije Universiteit.
^ Université de Haute-Alsace.

10.1021/jp062405x CCC: $33.50
Published on Web 08/26/2006

particular when they form hydrogen-bonded dimers in solution or in gas phase. This was observed for salicylic acid in aprotic polar media,[25] and in particular for 7-azaindole under a variety of circumstances.[26,27] The precise mechanism of ESDPT reactions and also the possible role they have in photoinduced mutagenesis are still under debate.[28,29]

The majority of studies on ESDPT involves the systems where the oxygen or nitrogen atom is both the hydrogen bond donor and the hydrogen bond acceptor.[30−33] The dimers of 7-azaindole or 1-azacarbazole[34,35] are typical representatives of this class. A significantly smaller amount of articles deals with mixed nitrogen−oxygen hydrogen-bonded systems that may be exemplified by alcohol complexes of 7-azaindole.[36] Recently, we investigated the nitramino pyridine *N*-oxides (NAPNO) series where a nitramino (−$NHNO_2$) group was substituted in the ortho-, meta-, or para-position with respect to the NO moiety.[37] In the solid phase, they occur as hydrogen-bonded dimers either in the normal (N) form (the hydrogen atom is at the amino nitrogen) or in a tautomeric proton transfer (PT) form where the H atom is at the NO group. Emissive properties of these compounds were not yet investigated, but instead quantum mechanical calculations at a semiempirical level (PM3) show that prototropic amino (N) ↔ imino (PT) equilibria may be present in solution and both forms could be encountered. Cyclic hydrogen-bonded dimers of the N form may be present in an apolar solvent, whereas more polar monomers of both species (N and PT) in conjunction with hydrogen-bonded PT dimers could occur in more polar environments. They also show interesting hydrogen-bonding networks. In the 2-nitramino-6-methylpyridine *N*-oxide dimer, for example, two parallel N monomers are linked by two intermolecular N−H···O hydrogen bonds of identical strength with an N−O distance of 2.711(2) Å. They are asymmetric and quasi-linear with an N−H···O angle of 172(2)°.[37]

In the presently investigated new series of methylated alkylamino nitropyridine *N*-oxides, the alkylamino (NHR) group occupies the ortho-position and the nitro group is in the para-position with respect to the NO group. In the solid state the title compound, 2-butylamino-6-methyl-4-nitropyridine *N*-oxide (2B6M), occurs as a doubly hydrogen-bonded dimer in the N form. It is composed of two internally hydrogen-bonded monomers, and the bifurcated and asymmetric three-centered hydrogen bond is formed of one intra- and one intermolecular N−H···O type interaction. The pyridine ring of 2B6M is planar and similar to alcohol complexes of 7-azaindole;[36] the hydrogen-bonding components are practically in the molecular plane.

The primary purpose of this work is to investigate the crystal structure of 2B6M, to perform an initial study of the photophysics of this compound, and to analyze electronic absorption and fluorescence spectra in a number of solvents. In addition, we want to compare experimental absorption spectra to calculated vertical excitation energies and oscillator strength values obtained from TD-DFT calculations for the ground state optimized structure and to discuss the amino−imino (N−H···O ↔ N···H−O) tautomerization from the point of view of experimental fluorescence spectra which will be compared to the results of semiempirical PM3 calculations involving excited-state structure optimization for the 2B6M and its tautomer.

On the basis of temperature-dependent absorption spectra of 2B6M in cyclohexane, we show that in apolar solvents we may deal with apolar dimers, while in polar solvents the more polar monomers are present. It is shown that in particular the emission spectra of 2B6M are very sensitive to solvent properties, and the large value of the Stokes shift (about 8000 cm^{-1}) in acetonitrile indicates an ESIPT reaction. Time-dependent fluorescence measurements showing two relaxation times corresponding to different spectral components confirm the presence of an excited-state proton-transfer reaction in polar solvents. This is in line with the findings from steady-state fluorescence measurements, which show the possibility of both forms (N and PT) being present in the excited state.

TABLE 1: Summary of Data Collection and Processing Parameters for the 2B6M Structure

chemical formula	$C_{11}H_{14}N_3O_3$
color/shape	orange/needles
formula weight	236.25
space group	$P\bar{1}$
temperature, K	100(1)
cell volume (Å^3)	550.2(5)
crystal system	triclinic
a (Å)	4.525(3)
b (Å)	10.096(4)
c (Å)	12.343(4)
α (deg)	77.72(4)
β (deg)	87.06(4)
γ (deg)	88.49(4)
formula units/unit cell	2
D_c (Mg m^{-3})	1.360
diffractometer/scan	Kuma KM-4 CCD/ω
radiation (Å) (graph monochromated)	0.71073
max crystal dimensions (mm)	0.231 × 0.211 × 0.093
θ range (deg)	27.99
range of h, k, l	0/10, 0/10, −30/28
reflections measured/independent	4627/2483 (R_{int} = 0.0428)
reflections observed $I > 2\sigma(I)$	1850
corrections applied	Lorentz and polarization effects
computer programs	CrysAlis RED,[38] SHELXTL 5.1[39]
structure solution	direct method
No. of parameters varied	151
weights[a] (a, b, f)	0.0637, 0, 1/3
GOF	1.065
$R_1 = \Sigma(\|F_o\| - \|F_c\|)/\Sigma(\|F_o\|)$	0.0455
$wR_2 = \{\Sigma[wF_o^2 - F_o^2)^2]/\Sigma[w(F_o^2)^2]\}^{1/2}$	0.0691
function minimized	$\Sigma w(\Delta F^2)^2$
largest feature final diff map (e Å^{-3})	0.308 and −0.211

[a] $a_w = 1/[\sigma^2(Fo^2) + (a\cdot P)^2 + b\cdot P]$ where $P = \times a6\cdot\max$ of (0 or F_o^2) + (1 − ×a6)·F_c^2.

Experimental Section

Synthesis. 2B6M was obtained by mixing equimolar amounts (0.01 mol) of 2-chloro-4-nitro-6-methylpyridine *N*-oxide and butylamine in a 40-cm^3 volume of ethanol. The mixture was then refluxed for 4 h, the ethanol was evaporated, water was added, and the precipitate was filtered off. Recrystallization from petroleum ether gave a 76% yield of 2B6M (mp 98 °C). Checked by GC/MS, the purity exceeds 99.9%. Elemental analysis shows its composition as follows: Calculated (%): C, 54.77; H, 6.90; N, 16.43. Found (%): C, 55.01; H, 6.88; N, 16.57. Ethanol and petroleum ether used for the synthesis were of analytical grade. The compound dissolves well in organic solvents and water.

X-ray Structure. A crystal suitable for X-ray diffraction was grown from a binary mixture of methanol and water (3:1). Orange needles appeared after a few days. Intensity data collection was carried out on a KUMA KM4 κ-axis diffractometer equipped with a CCD camera and an Oxford Cryo-system. All data were corrected for Lorentz and polarization effects. Data reduction and analysis were carried out with the KUMA diffraction programs.[38] The structure was solved by the direct methods and refined by the full-matrix least-squares method on F^2 data using the SHELXTL (version 5.1) program.[39] Experimental details are summarized in Table 1.

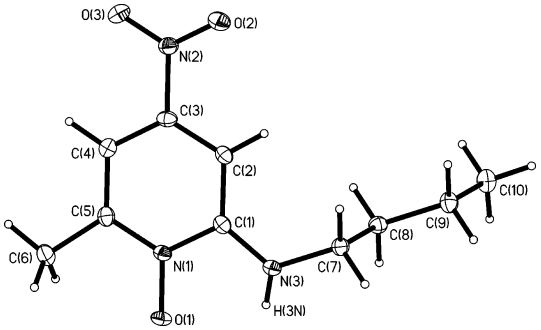

Figure 2. ORTEP diagram of 2B6M showing crystallographic labeling. Thermal ellipsoids are drawn at the 50% probability level.

Electronic Absorption Spectra. Electronic absorption spectra in solution were recorded on a CARY-1 UV−vis spectrometer in the concentration range 10^{-3} to 10^{-5} M. The solvents used in all absorption and emission experiments (hexane, cyclohexane, toluene, diethyl ether, ethyl acetate, tetrahydrofuran, and acetonitrile) were of spectroscopic grade and used as purchased (Merck, Uvasol). Acetonitrile was dried over a molecular sieve prior to use.

Steady-State Emission Spectroscopy. Emission spectra were recorded on a Perkin-Elmer LS-50B fluorimeter and on an FSL900 luminescence setup of Edinburgh Instruments Ltd. For the emission spectra, the optical density was kept at ∼0.2 (path length 1 cm) to avoid reabsorption and inner filter effects. Spectra were corrected for detector response and excitation source. The concentration of the solutions was about 10^{-5} M.

Time-Resolved Fluorescence Spectroscopy. Lifetimes of 2B6M were measured in solution (10^{-5} M) using the time-correlated single-photon counting technique.[40] The excitation source was a Coherent Mira 900 Ti:Sapphire laser with a pulse width of ∼3 ps. The laser output was frequency tripled to obtain the excitation wavelength of 295 nm. The energy was $\sim 10^{-2}$ nJ/pulse. Fluorescence was collected from the sample at right angles through an optical system and dispersed by a spectrometer on an MPP-PMT (Hamamatsu R3809U-50) detector. Decay data were recorded with the help of an SPC-630 (Becker-Hickl) module and analyzed using Fluofit software (Picoquant). In all cases, a good fit was obtained with a reduced χ^2 close to unity and residuals distributed normally.[41] The accuracy of the instrument was checked by recording the lifetimes of some standard compounds. Reproducibility of the lifetimes was around 50 ps. The temperature was controlled and measured in a home-built system. The precision in temperature was about 1 K.

Theoretical Calculations. Ground-state optimization of 2B6M was performed at the [B3LYP/6-31G (d, p)] level with Gaussian 98.[42] Vertical excitation energies and oscillator strengths were calculated by the TD-DFT [B3LYP/6-31G(d, p)] method.[42] Additionally, for comparison purposes, full geometry ground- and excited-state optimization of the N and PT forms of 2B6M, as well as calculation of their absorption and emission spectra, was performed by means of semiempirical PM3 calculations.[43,44] Theoretical vertical transition energies for absorption and emission in hexane and acetonitrile for the N and PT forms were calculated on the basis of the solvent effect theory.[45,46]

Results and Discussion

X-ray Structure. The X-ray crystal structure of 2B6M is presented in Figures 2 and 3. Atom coordinates, bond lengths, valence angles, dihedral angles, and other crystallographic data were deposited at the Cambridge Crystallographic Data Center CCDC No. 286564.

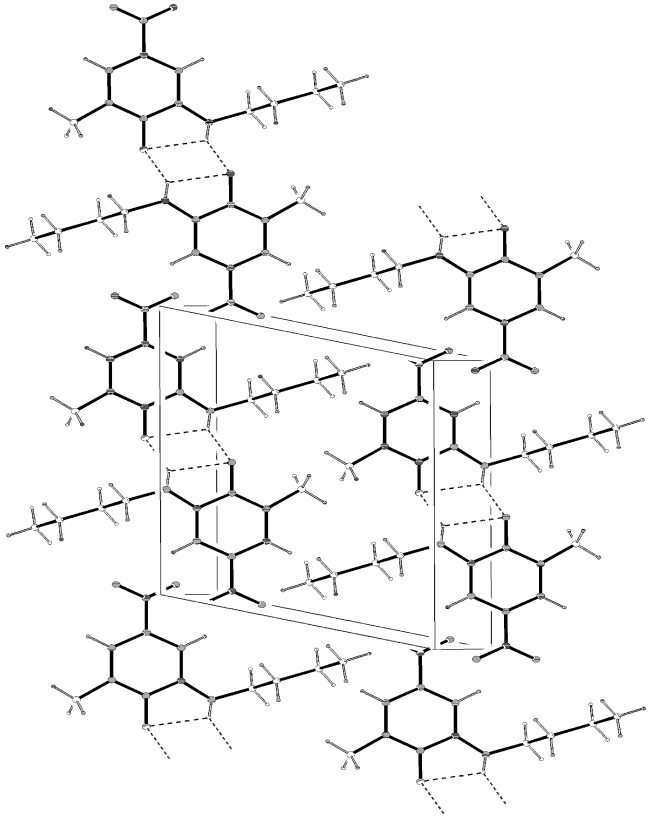

Figure 3. Crystal packing of 2B6M.

TABLE 2: Comparison of X-ray Data of 2B6M with Those of the 2-Nitramino-6-methylpyridine *N*-Oxide[37] and 2-Nitramino-3-methylpyridine *N*-Oxide[47] Structures[a]

parameter	2B6M(H)	6M(H)[37]	3M(H)[47]
displacement of the NO group (deg)	0.4(2)	−177.8(2)	−177.3(1)
d(N−O)$_{NO}$ (Å)	1.3149(17)	1.319(2)	1.316(2)
displacement of the $N_{(amino)}$ atom (deg)	−179.23(13)	177.2(2)	175.3(2)
d(C_{ar}−N_{amino}) (Å)	1.343(2)	1.409(2)	1.410(2)
displacement of the NO_2 group (deg)	−179.29(14)	70.6(2)	−70.8(3)
d(C_{ar}−C_{Me}) (Å)	1.490(2)	1.479(3)	1.491(2)

[a] Both molecules are in the amino form in the crystal structure.

We limit our discussion of the crystal structure to a brief comparison with the recently studied NAPNO compounds and to the hydrogen-bonding geometry of the solid 2B6M dimer.

As shown in Figure 3, 2B6M crystallizes in the form of a double hydrogen-bonded dimer, which consists of two internally hydrogen-bonded monomers. The oxygen atom of the NO group and the hydrogen atom of the amine group of each monomer contribute simultaneously to an intra- (2.556(2) Å) and an intermolecular (2.891(3) Å) N−H···O type hydrogen bond. Due to the weak C−H···$O_{(NO2)}$ (3.472(3) Å) contact interactions that take place between adjacent dimeric units, a chainlike single layer of dimers is formed. The oxygen atom, in this case, does not originate from the NO group of a parent molecule but from the nitro group of the neighboring *N*-oxide molecule.

The distance that separates mutually parallel planes of monomers in a double layer of dimers is relatively short (3.049-(3) Å), which may be a reason for stacking and excitonic interactions visible in the form of band splitting in the absorption spectrum in nonpolar solvents.

Comparative X-ray data of Table 2 show that, similar to our previously studied methylated NAPNO structures,[37] the pyridine

TABLE 3: Hydrogen Bonds in 2B6M Dimer (Å and Deg)

D−H···A	*d*(D−H)	*d*(H···A)	(D···A)	<(DHA)
N(3)−H(3N)···O(1)	0.83(2)	2.15(2)	2.556(2)	110(2)
N(3)−H(3N)···O(1)#1	0.83(2)	2.19(2)	2.891(3)	143(2)
C(2)−H(2A)···O(2)#2	0.95	2.54	3.472(3)	167

ring of 2B6M is entirely planar and all functional groups that might participate in proton transfer (NO, NHR, NO_2) are situated in the molecular plane. This finding is confirmed by the values of the appropriate O1−N1−C1−C2 (0.4(2)°), C5−N1−C1−N3 (−179.23(13)°), and C5−C4−C3−N2 (−179.29(14)°) dihedral angles, which makes 2B6M indeed a potential candidate for an ESIPT reaction.

The fact that 2B6M crystallizes in the amino and not in the imino form seems to result from a prevailing inductive effect of butyl group over the mesomeric effect of the nitro group. The C_{ar}−N_{amino} distance (1.343(2) Å) is substantially shortened in comparison to the previously studied methylated NAPNO compounds 1.410(2) Å[47] or 1.360(3) Å.[48]

Hydrogen Bonding. On the basis of the crystal structure, we can conclude that the hydrogen bond donors and acceptors of 2B6M participate in so-called "bifurcated, four-centered interactions".[49] The hydrogen atom of the amino group in each monomer of the dimer is surrounded by three other electronegative atoms. As shown in Figure 3 and Table 3, two of these atoms, that is, the amino nitrogen, N(3), and the nitroso oxygen, O(1), belong to the same molecule, while the third one, O(1)#1, is located at the neighboring *N*-oxide molecule. In this way, the hydrogen atom of each amino group participates in one intramolecular and one intermolecular hydrogen bond of the same type. A squarelike system is composed of four almost equal H···O(NO) distances, two of them (2.15(2) Å) originating from two intramolecular bonds, and the other two (2.19(2) Å) originating from intermolecular N−H···O bonds. Both types of hydrogen bond are asymmetric and angular, and the N−H distances for the intra- and intermolecular hydrogen bonds are the same (0.83(2) Å), while the NHO valence angles are 110-(2)° and 143(2)°, respectively.

The intramolecular hydrogen bond seems to be slightly stronger when compared to the N···O distances of 2.67 and 2.615 Å found in internally hydrogen-bonded benzoxazoles.[50,51] However, the distance between the proton donor (N−H) and proton acceptor (H···O) atom, 2.15(2) Å, falls in the range of 1.5−2.2 Å, characteristic of stronger hydrogen bonds found in many biological systems.[52] They are significantly shorter than the distances calculated from the van der Waals contacts for the N···O heavy atoms (2.9 Å).[53]

Absorption: Polarity Effects. Similar to most other compounds that exhibit excited-state proton-transfer reactions, the photophysics of 2B6M is complex and shows a strong dependence on the solvent used. The compound gives, in all solvents studied, a series of broad absorption bands, of which the structure depends on the solvent (Figure 4). In polar solvents (such as acetonitrile), the bands are broad and smooth with absorption below 500 nm; in apolar solvents, the absorption starts more to the blue and some more structure is seen, which could be vibrational, in line with what is usually observed in apolar, aprotic solvents. The observed splittings of the bands are between ∼1150 cm^{-1} (bands around 280 nm) and ∼1350 cm^{-1} (bands at 430 nm).

To try to resolve the origin of the band splitting in the absorption spectrum of 2B6M in apolar solvents, as displayed in Figure 4, concentration (10^{-3} to 10^{-5} M) and temperature (25−80 °C) dependence studies were carried out. The concentration-dependent spectra show only very minor changes, but the temperature-dependent spectra, when corrected for the temperature dependence of the density of the solvent, show most clearly in the difference spectra (Figure 5) a number of isosbestic points that can be taken as an indication that two species are present. On the basis of these data, we can calculate the energy difference between these species, assuming Arrhenius behavior. This gives an energy difference of approximately 1200 cm^{-1}, which is far too small (see Theoretical Calculations) to be explained by the presence of the ground-state tautomer. We therefore assume that we are indeed dealing with dimers, and the large energy difference explains why no changes are

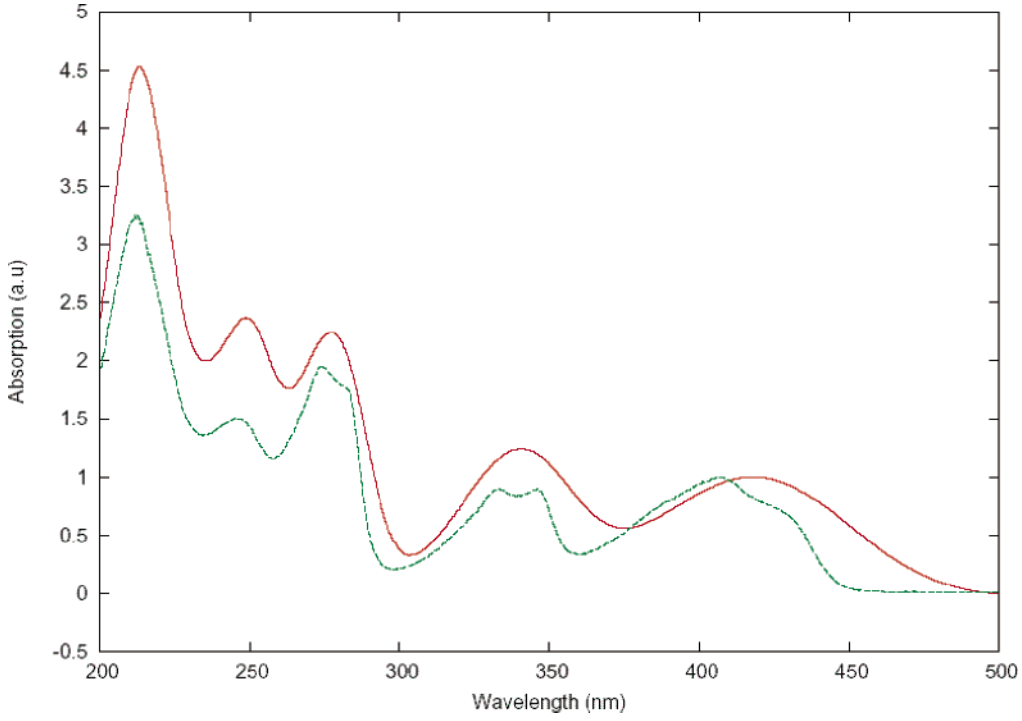

Figure 4. Absorption spectrum in acetonitrile (red curve) and in hexane (green curve).

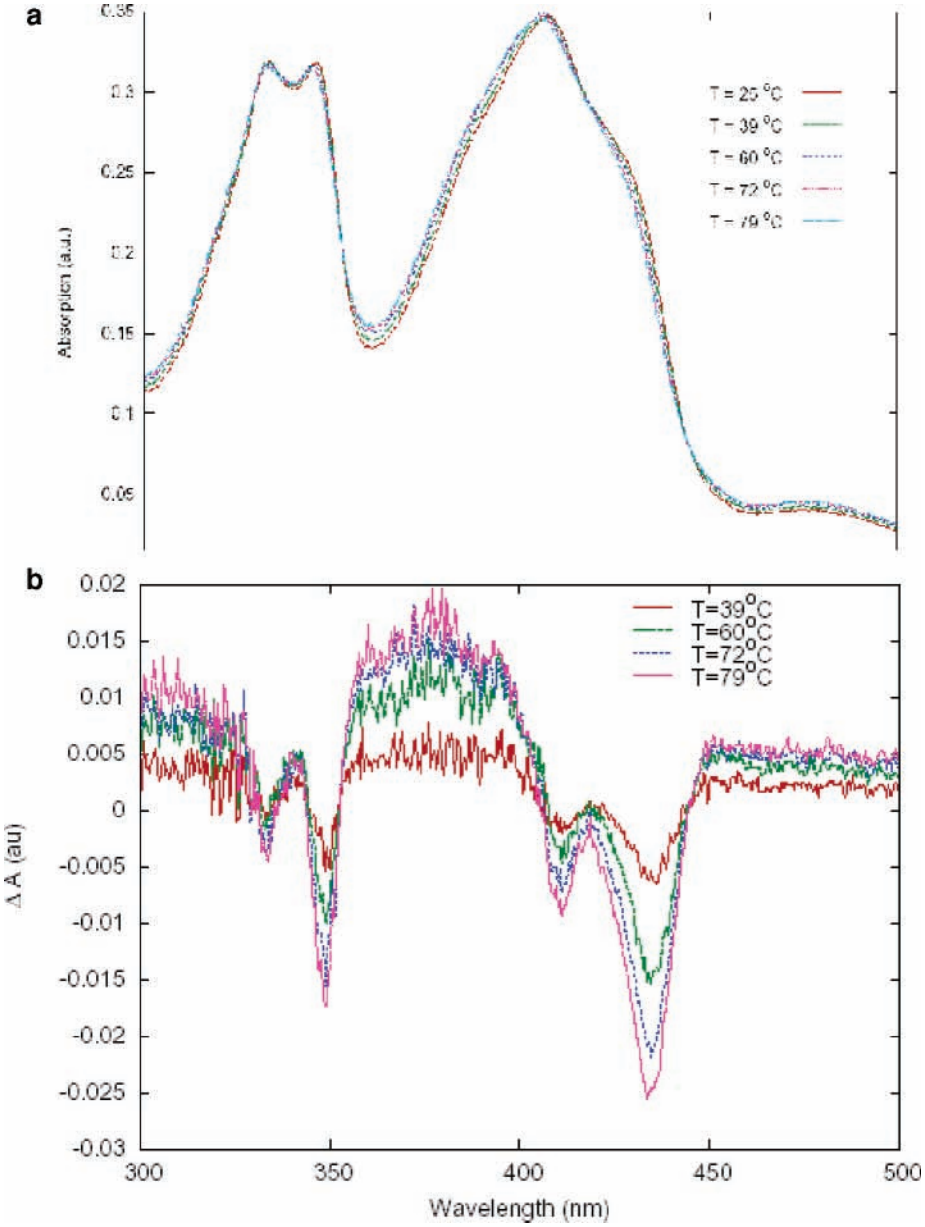

Figure 5. Temperature-dependent normal (a) and difference (b) absorption spectra of 2B6M in cyclohexane. Difference spectra are in respect to the spectrum at 25 °C. The concentrations were corrected for density changes of the solvent.

observed for different concentrations: based on an equilibrium constant with the above energy difference, concentrations at which we expect monomers to be present in an appreciable amount would have too low absorbance to measure. The splitting in the spectra is then due to excitonic interaction in the dimer.

In fact, two types of dimer are possible: the double hydrogen-bonded dimer also found in the crystal structure and a stacked dimer also found in the crystal structure, since the distance between molecular planes of monomers, in particular layers of dimers in the crystal lattice, is very short (3.04 Å). An estimate of the excitonic interaction based on the calculated oscillator strength (see below) for this distance would be ~850 cm^{-1}, which does give the right order of magnitude for the splitting.

Fluorescence: Polarity Effects. The fluorescence spectra show even more variation. Absorption maxima change very little (i.e., merely ca. 10 nm on going from cyclohexane to acetonitrile), while the emission maximum is strongly affected by dielectric permittivity of the solvent. Figure 6 displays fluorescence spectra of 2B6M in a number of solvents of varying polarity and hydrogen-bonding ability. Spectra vary greatly in intensity and position. Some of the measured parameters are reported in Table 4.

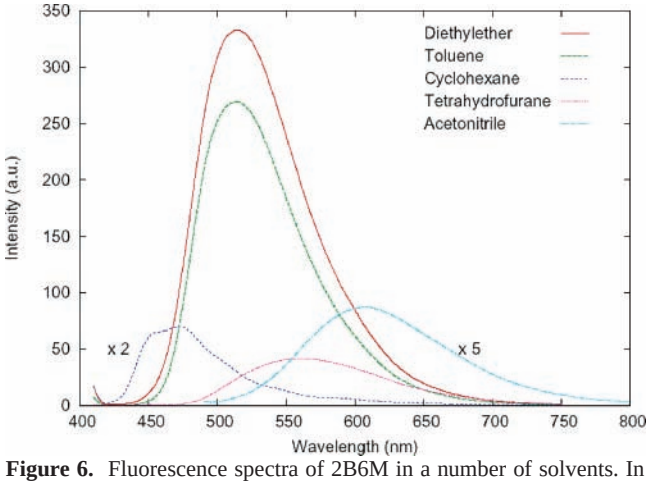

Figure 6. Fluorescence spectra of 2B6M in a number of solvents. In acetonitrile the excitation wavelength was 420 nm, and in all other cases it was 400 nm. Concentration: 10^{-5} M.

TABLE 4: Absorption Maxima (Redmost Maximum), Fluorescence Maxima, and Stokes Shift Values of 2B6M in a Number of Solvents[a]

solvent	dielectric permittivity	absorption maximum (nm)	fluorescence maximum (nm)	$\Delta\nu_{ST}$ (cm^{-1})
cyclohexane	2.02	406	473	3859
toluene	2.38	407	514	5545
diethyl ether	4.34	410	515	5583
ethyl acetate	6.09	416	567	7364
tetrahydrofuran	7.52	421	570	7457
acetonitrile	38.8	420	620	7680

[a] For the fluorescence maxima excitation was at 400 nm (420 nm in acetonitrile); concentrations 10^{-5} M. Dielectric permittivity values taken from ref 45.

It is worthwhile to note that with solvent polarity increase the value of the Stokes shift also increases significantly: whereas in cyclohexane ($\epsilon = 2.02$) it is 3859 cm^{-1}, in the strongly polar acetonitrile ($\epsilon = 38.8$) it is almost twice that value (7680 cm^{-1}). Such spectral behavior strongly indicates significant structural changes of 2B6M in the excited state and large value of dipole moment of the emitting form with respect to the ground-state species. On the basis of this observation, we may postulate that excited-state intramolecular proton-transfer reaction is likely to take place in polar solvents, which will be further shown below by the results of the corresponding quantum mechanical calculations.

In apolar aprotic solvents, the situation seems to be more complex. For instance, in hexane, apart from the main maximum at about 470 nm, a shoulder and at least two additional peaks of a weak intensity (540−650 nm) appear on the red side of the fluorescence spectrum. One of them coincides with the emission maximum of the solid 2B6M, also presented in Figure 7, which has a peak at 560 nm that could be assigned to an excited-state double proton-transfer band. Again the excitonic model with the stacking configuration would give an explanation for the very weak fluorescence, since for that configuration the lowest energy state would be dark.

Lifetimes. Unfortunately, the signal of the fluorescence emission in cyclohexane and other aprotic, apolar solvents was too small to perform accurate lifetime measurements. Time-resolved data taken in other solvents show that in general two lifetimes are found, which are reported for toluene, acetonitrile, and ethyl acetate in Table 5. We note that the wavelength dependence of the amplitudes reported in that table shows that two separate spectral components are present, of which the lifetime does not vary much, where in the case of ethyl acetate and toluene the redmost component has the longest lifetime, whereas in acetonitrile it has the shorter lifetime. We see no in-growth of the spectra for very short times, which is in line with the fact that ESIPT is supposed to take place very rapidly also for this compound,[54] leading to a quick equilibrium between the excited-state species.

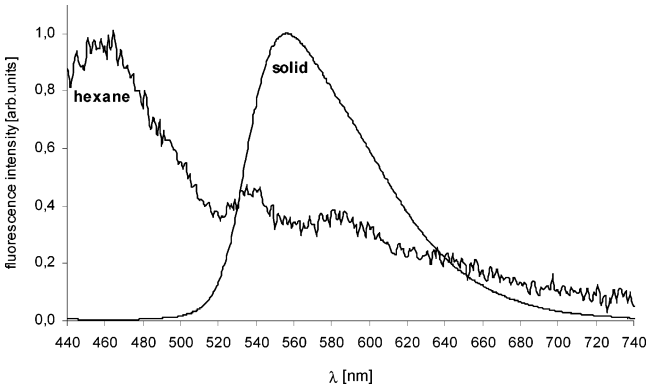

Figure 7. Fluorescence spectrum of the solid 2B6M overlaid on the fluorescence spectrum in hexane.

TABLE 5: Decay Lifetimes of 2B6M in Different Solvents Observed at Different Emission Wavelengths; Excitation at 291 nm

solvent	λ_{em} (nm)	decay times (ns) and amplitudes (%)	ξ^2
toluene	570	$\tau_1 = 2.18$ (100)	1.0
	550	$\tau_1 = 2.17$ (90.4)	1.3
		$\tau_2 = 0.37$ (9.6)	
	530	$\tau_1 = 2.15$ (90.2)	1.3
		$\tau_2 = 0.59$ (9.8)	
	510	$\tau_1 = 2.15$ (83.1)	1.3
		$\tau_2 = 0.51$ (16.9)	
	490	$\tau_1 = 2.13$ (80.0)	1.2
		$\tau_2 = 0.47$ (20.0)	
ethyl acetate	630	$\tau_1 = 2.48$ (100)	1.5
	600	$\tau_1 = 2.47$ (91.1)	1.4
		$\tau_2 = 0.9$ (8.9)	
	570	$\tau_1 = 2.48$ (86.9)	1.4
		$\tau_2 = 0.8$ (13.1)	
	520	$\tau_1 = 2.51$ (76.6)	1.4
		$\tau_2 = 0.49$ (23.4)	
CH_3CN	620	$\tau_1 = 1.25$ (0.18)	1.4
		$\tau_2 = 0.14$ (99.82)	
	610	$\tau_1 = 1.31$ (0.2)	1.4
		$\tau_2 = 0.14$ (99.8)	
	600	$\tau_1 = 1.16$ (0.4)	1.2
		$\tau_2 = 0.14$ (99.6)	

TABLE 6: Ground-State DFT [(B3LYP/6-31G (d, p)] Optimized Structure of 2B6M Compared to Experimental X-ray Data[a]

bond	expt (Å)	calcd (Å)
O(1)−N(1)	1.3149(17)	1.293
O(2)−N(2)	1.2263(18)	1.233
O(3)−N(2)	1.2228(18)	1.232
N(1)−C(5)	1.363(2)	1.372
N(1)−C(1)	1.382(2)	1.397
N(2)−C(3)	1.474(2)	1.463
N(3)−H(3N)	0.69(3)	1.016
N(3)−C(1)	1.343(2)	1.348
N(3)−C(7)	1.459(2)	1.451
C(1)−C(2)	1.400(2)	1.394
C(1)−H(3N)	1.63(3)	1.976
C(2)−C(3)	1.370(2)	1.390
C(3)−C(4)	1.381(2)	1.390
C(4)−C(5)	1.377(2)	1.387
C(5)−C(6)	1.490(2)	1.490
C(7)−C(8)	1.524(2)	1.531
C(7)−H(3N)	1.98(3)	2.170
C(8)−C(9)	1.520(2)	1.537
C(9)−C(10)	1.522(2)	1.533

[a] Atom labeling as in Figure 2.

Theoretical Calculations. Full DFT optimization at the [B3LYP/6-31G(d, p)] level mostly correctly reproduces the experimental structure of 2B6M shown in Table 6. The experimental H(N3)···O(1) (2.15(2) Å) and N(3)···O(1) (2.556 (2) Å) distances agree well with those calculated at 2.013 and 2.538 Å, respectively. The experimental N(3)−H(3N) distance 0.83(2) Å is, however, different from the calculated value of 1.016 Å.

These discrepancies may result from the fact that only the monomeric unit was optimized while in the solid state the 2B6M occurs in the form of the hydrogen-bonded dimer. The optimized ground-state geometries of the normal and tautomeric form suggest that rather large geometrical changes may accompany the proton-transfer reaction of 2B6M in the excited state,

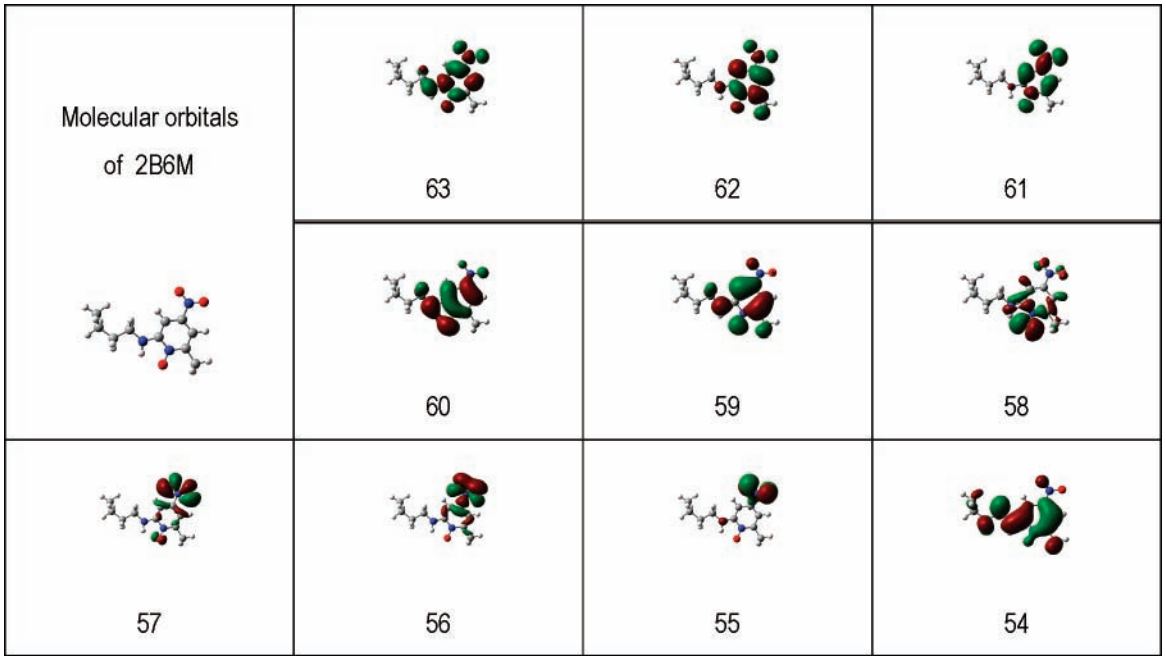

Figure 8. Frontier molecular orbitals of 2B6M contributing to the $S_0 \leftrightarrow S_i$ transitions. (TD DFT method at the B3LYP/ 6-31G** level.)

TABLE 7: Transition Energies, Oscillator Strengths, and the Character of $S_0 \rightarrow S_i$ Transitions in 2B6M[a]

state	transition energy ΔE (nm)	transition energy ΔE (cm^{-1})	oscillator strength F	character of transition
1	417.0	23983	0.071	60 → 61
2	341.6	29275	0.000	58 → 61 57 → 61
3	326.9	30592	0.000	57 → 61 58 → 61
4	321.7	31081	0.115	59 → 61
5	292.4	34196	0.000	56 → 61
6	265.1	37716	0.123	60 → 62
7	237.1	42185	0.158	60 → 63
8	224.3	44577	0.013	54 → 61
9	220.8	45286	0.000	58 → 62
10	215.0	46505	0.022	55 → 61

[a] TD-DFT calculations on the [B3LYP/6-31G (d, p)] level.

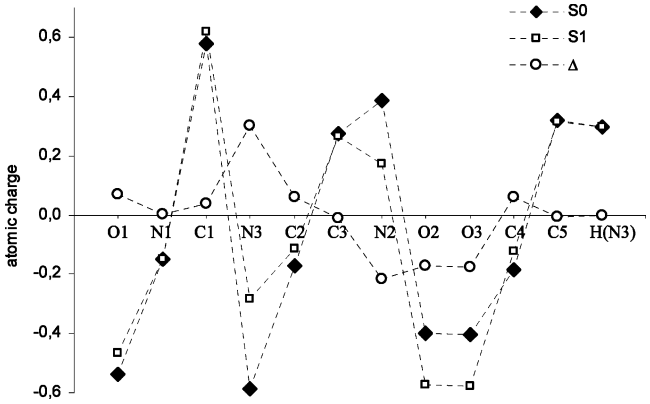

Figure 9. Charge distribution in the ground (S_0) and excited (S_1) states of the N form of 2B6M (DFT calculations).

including indeed a loss of aromaticity. Neither the C−C ring bonds nor the $C(1)-N_{NO}$ (1.4132 Å) and $C(5)-N(1)_{NO}$ (1.3509 Å) bonds have the same length, while the $C(3)-N(2)_{NO2}$ bond is slightly elongated (0.0192 Å.). It could rather represent a sort of quinoidal-like structure.[55,56] Such geometry changes are deemed to be important and are claimed to play the large role in the PT dynamics, even providing the driving force for the ESIPT reaction.

The TD-DFT [B3LYP/6-31G(d, p)] calculated electronic absorption spectra, with all theoretical $S_0 \rightarrow S_i$ transitions, are displayed in Table 7. Generally, the calculated electronic transitions presented in Table 7 reproduce experimental findings well, although the first calculated absorption maximum is slightly red-shifted 23 983 cm^{-1} (417 nm) with respect to the experimental value of 24 630 cm^{-1} (406 nm). The dominating contribution to the $S_0 \rightarrow S_1$ transition is derived from HOMO → LUMO electronic configurations. These two molecular orbitals of 2B6M are displayed in Figure 8.

It is seen that the $S_0 \rightarrow S_1$ transition is of $\pi \rightarrow \pi^*$ type and is connected with a certain shift of charge from the electron donors to the nitro group. This is also illustrated in Figure 9, where the charge distributions on particular atoms of 2B6M in the ground (S_0) and the excited (S_1) states are presented.

It can also be inferred from Figure 9 that the $S_0 \rightarrow S_1$ transition favors an ESIPT reaction. It is obvious that, upon electronic excitation, excess electron density on the nitrogen atom (N3) of the amine group shifts to the nitro group. As a result, the acidity of the amino nitrogen increases so that its hydrogen is more easily transferred into the direction of the NO group. ESIPT in 2B6M is further discussed below on the basis of the results of semiempirical PM3 calculations presented in the form of a diagram in Figure 10. Within the framework of these calculations, both the N and PT species were optimized in their ground (S_0) and lowest excited (S_1) electronic states. The transition energies and dipole moments calculated for the species are displayed in Figure 10. According to the results of these calculations (which correspond to the 2B6M in the gas phase), the N form in the ground electronic state (S_0) is far more stable (by ca. 5700 cm^{-1}) than the PT form. The dipole moment of the N-form in the ground state is 3 D, while the dipole moment of the PT form is 3.6 D. Vertical transition energies to the Franck−Condon S_1 states are 25 650 and 22 260 cm^{-1}, respectively. The value 25 650 cm^{-1} agrees well with the experimental value of 24 630 cm^{-1} for absorption. The dipole moments corresponding to the FC S_1 states are larger than those in the ground state: 5.3 and 7.8 D for the N and PT forms, respectively.

Similar calculations for both forms optimized in the S_1 state show that the N form is more stable by ca. 500 cm^{-1}. It is

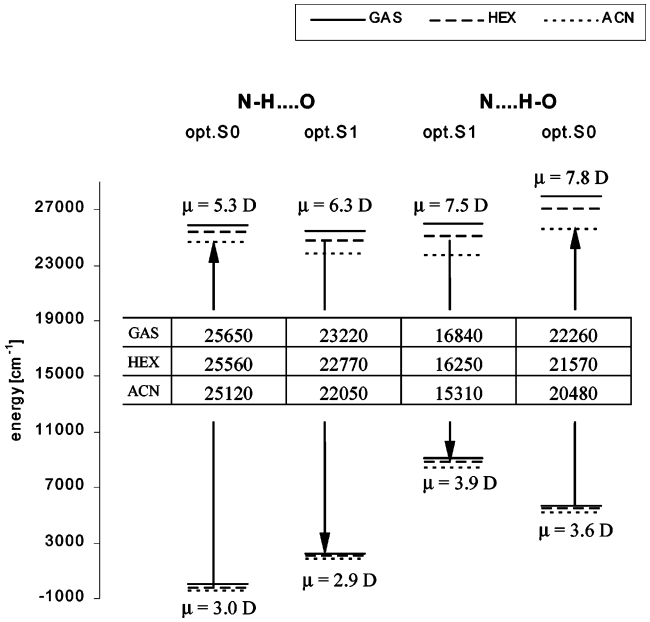

Figure 10. Relative stability of the normal (N−H···O) and PT (N···HO) forms (see text) of 2B6M in the gas phase and in two different solvents. Appropriate values of transition energy in the gas phase (Gas), hexane (HEX), and acetonitrile (ACN) are presented in the inserted table. (MOPAC-PM3 (MECI, CI = 6) calculations).

characterized by a dipole moment of 6.3 D and transition energy to the S_0 state (fluorescence) as 23 220 cm^{-1}, while the corresponding values for the PT form are 7.5 D and 16 840 cm^{-1}, respectively. This energy difference is consistent with the presence of both the N and PT forms in the excited state.

On the basis of these calculations, we expect that the N form of 2B6M is the absorbing (at 25 650 cm^{-1}) as well as the emitting (at 23 220 cm^{-1}) species in the gas phase. However, this picture can change for 2B6M in solution (especially in polar solutions) because in general the PT form is more polar than the N form. The energies of the electronic states of molecule interacting with a solvent can be estimated[57,58] by means of the following expressions:

For the optimized ground electronic state S_0:

$$E_s(S_0) = E_g(S_0) - \mu^2(S_0)f_\epsilon$$

For the FC excited electronic state S_1^{FC}:

$$E_s(S_1^{FC}) = E_g(S_1^{FC}) - \mu^2(S_1^{FC})f_n - \mu(S_1^{FC})\mu(S_0)(f_\epsilon - f_n)$$

For the optimized excited electronic state S_1:

$$E_s(S_1) = E_g(S_1) - \mu^2(S_1)f_\epsilon$$

Finally, for the FC ground electronic state S_0^{FC}:

$$E_s(S_o^{FC}) = E_g(S_o^{FC}) - \mu^2(S_0^{FC})f_n - \mu(S_0^{FC})\mu(S_1)(f_\epsilon - f_n)$$

In these equations, f_ϵ and f_n are the solvent functions:

$$f_\epsilon = (2/hca^3)[(\epsilon - 1)/(2\epsilon - 1)] \quad \text{and}$$

$$f_n = (2/hca^3)[(n^2 - 1)/(2n^2 - 1)]$$

where ϵ is the dielectric constant and n is the refractive index of the solvent. The Onsager cavity radius a was estimated as 0.4 of the longest molecular axis. $E_g(S_0)$, $E_g(S_1^{FC})$, $E_g(S_1)$, and $E_g(S_o^{FC})$ are the energies in the gas phase of the ground state, FC excited state, excited equilibrated state, and FC ground state, respectively, whereas $\mu(S_0)$, $\mu(S_1^{FC})$, $\mu(S_1)$, and $\mu(S_o^{FC})$ are the dipole moments of these states.

The energy difference

$$\Delta_a = E_s(S_1^{FC}) - E_s(S_1)$$

corresponds to the transition energy for the absorption $S_0 \rightarrow S_1^{FC}$, and

$$\Delta_f = E_s(S_1) - E_s(S_0^{FC})$$

corresponds to the transition energy for the emission $S_1 \rightarrow S_0^{FC}$.

Using these expressions, we have calculated energies of the states of both forms of 2B6M in solvents of different polarity. Results of these calculations are shown in Figure 10. It is seen that in the apolar hexane the arrangement of the states is similar to that described earlier for the gas phase (i.e., the N form is more stable than the PT form in both electronic states with predicted shift of the absorption band to 25 560 cm^{-1} and the fluorescence band to 22 770 cm^{-1}). More interesting results are obtained for polar solutions such as acetonitrile. We see that in this case the reversion of the arrangement of excited S_1 states takes place. The PT form in the S_1 state becomes more stable than the N form. This is an indication that ESIPT can take place in 2B6M: upon excitation of the N form (at 25 100 cm^{-1}) the PT form in the S_1 state is populated from S_1^{FC}. The transition energy for fluorescence of the PT form in acetonitrile is predicted at 15 310 cm^{-1}. This is in reasonable accordance with experimental value of 16 000 cm^{-1} for the maximum of the broad emission band of 2B6M in acetonitrile.

Conclusions

On the basis of the X-ray diffraction, we resolved the crystal structure of 2-butylamino-6-methyl-4-nitropyridine *N*-oxide (2B6M), the first representative of a newly synthesized series of alkyl amino derivatives of 4-nitropyridine *N*-oxide. In the crystal structure, hydrogen bonding is both intramolecular between the amino hydrogen atom and the oxygen of the NO group as well as intermolecular to a neighboring molecule. The intramolecular hydrogen bond of 2B6M makes it a likely candidate for phototautomerization.

An initial study of its photophysical properties was performed by a combination of experimental and quantum theoretical methods. From the temperature-dependent difference absorption spectra in hexane we concluded that in apolar solvents a dimeric species is most likely, where the fluorescence is too weak to experimentally probe the possibility of ESDPT, of which there is some indication in the emission spectra. Fluorescence decay investigations of ESIPT of 2B6M were carried out in polar media where the monomeric species is prevalent. On the basis of the experimental and theoretical evidence described in this article, 2B6M in polar media exhibits an ESIPT reaction where both the N and PT forms appear to be present and emit in the excited state. This is corroborated by both the strongly red-shifted fluorescence emission band corresponding to the PT species with a Stokes shift of about 8000 cm^{-1} (in acetonitrile) and the dual fluorescence decays which can be related to different spectral components.

TD-DFT calculated vertical excitation energies nicely reproduce the experimental absorption maxima in nonpolar solvents, and those calculated by the semiempirical PM3 method on the S_1 optimized structures are in agreement with the experimental fluorescence maxima in acetonitrile. Results of the PM3

calculation also indicate that ESIPT can take place in the 2B6M molecule and that the calculated energy difference indeed allows the presence of both species in the excited state at room temperature.

The variation of the Stokes shift as a function of polarity and the presence of two tautomeric forms in the excited state make the compound a suitable candidate as a polarity probe. A more thorough investigation of the photophysical properties in other solvents and solvent mixtures should give more insight into these possibilities. The biological activity of 2B6M and the crystal structure and photophysics of other alkylamino derivatives of 4-nitropyridine *N*-oxide are currently under investigation.

Acknowledgment. A.S.-H. greatly acknowledges the support of the European Community-Access to Research Infrastructures Action of The Improving Human Potential (Contract No. HPRI-CT-1999-00064) for performing part of these studies in the Laser Center of the Free University of Amsterdam (The Netherlands) as well as an internal grant of the Faculty of Chemistry of the University of Wrocław.

References and Notes

(1) Burkus, J. *J. Org. Chem.* **1962**, *27*, 474.
(2) Hagiwar, H.; Inoguchi, H.; Fukushima, M.; Hoshi, T.; Suzuki, T. *Synlett* **2005**, *15*, 2388.
(3) Malkov, A. V.; Bell, M.; Castelluzzo, F.; Kocovsky, P. *Org. Lett.* **2005**, *7*, 3219.
(4) Chelucci, G.; Murineddu, G.; Pinn, G. A. *Tetrahedron: Asymmetry* **2004**, *15*, 1373.
(5) Nantermet, P. G.; Burgey, C. S.; Robinson, K. A.; Pellicore, J. M.; Newton, C. L.; Deng, J. Z.; Selnick, H. G.; Lewis, S. D.; Lucas, B. J.; Krueger, J. A.; Miller-Stein, C.; White, R. B.; Wong, B.; McMasters, D. R.; Wallace, A. A.; Lynch, J. J.; Yan, Y. W.; Chen, Z. G.; Kuo, L.; Gardell, S. J.; Shafer, J. A.; Vacca, J. P.; Lyle, T. A. *Bioorg. Med. Chem. Lett.* **2005**, *15*, 2771.
(6) Pool, J. A.; Scott, B. L.; Kiplinger, J. L. *Chem. Commun.* **2005**, *20*, 2591.
(7) Pool, J. A.; Scott, B. L.; Kiplinger, J. L. *J. Am. Chem. Soc.* **2005**, *127*, 1338.
(8) Balzarini, J.; Stevens, M.; De Clercq, E.; Schols, D.; Pannecouque, C. *J. Antimicrob. Chemother.* **2005**, *55*, 135.
(9) Yousif, S. *ARKIVOC* **2001**, 242.
(10) Soscun, H.; Castellano, O.; Bermudez, Y.; Toro-Mendoza, C.; Marcano, A.; Alvarado, Y. *J. Mol. Struct.: THEOCHEM* **2002**, *592*, 19.
(11) Eaton, D. F. *Science* **1991**, *253*, 281.
(12) Iba, N. M.; Nguyen, T.; Fung, J. *Arch. Biochem. Biophys.* **2002**, *404*, 326.
(13) Weller, A. *Naturwissenschaften* **1955**, *42*, 175.
(14) Weller, A. *Z. Elektrochem.* **1956**, *60*, 1144.
(15) Weller, A. *Prog. React. Kinet.* **1961**, *1*, 187.
(16) Joshi, H. C.; Gooijer, C.; van der Zwan, G. *J. Phys. Chem. A* **2002**, *106*, 11422.
(17) Joshi, H. C.; Gooijer, C.; van der Zwan, G. *J. Fluoresc.* **2003**, *13*, 227.
(18) Smoluch, M.; Joshi, H.; Gerssen, A.; Gooijer, C.; van der Zwan, G. *J. Phys. Chem. A* **2005**, *109*, 535.
(19) Bader, A. N.; Ariese, F.; Gooijer, C. *J. Phys. Chem. A* **2002**, *106*, 2844.
(20) Chou, P.; Aartsma, T. J. *J. Phys. Chem.* **1986**, *90*, 721.
(21) McMorrow, D.; Dzugan, T. P.; Aartsma, T. J. *Chem. Phys. Lett.* **1984**, *103*, 492.
(22) Klymchenko, A. S.; Demchenko, A. P. *J. Am. Chem. Soc.* **2002**, *124*, 12372.
(23) Hynes, J. T.; Tran-Thi, T.-H.; Granucci, G. *J. Photochem. Photobiol.* **2002**, *154*, 3.
(24) Kosower, E. M.; Huppert, D. *Annu. Rev. Phys. Chem.* **1986**, *37*, 127.
(25) Pant, D. D.; Joshi, H. C.; Bisht, P. B.; Tripathi, H. B. *Chem. Phys.* **1994**, *185*, 137.
(26) Catalan, J.; Perez, P.; del Valle, J. C.; de Paz, J. L. G.; Kasha, M. *Proc. Natl. Acad. Sci. U.S.A.* **2002**, *99*, 5793.
(27) Douhal, A.; Moreno, M.; Lluch, J. M. *Chem. Phys. Lett.* **2000**, *324*, 75.
(28) El-Kemary, M. A.; El-Gezawy, H. S.; El-Baradie, H. Y.; Issa, R. M. *Chem. Phys.* **2001**, *265*, 233.
(29) Folmer, D. E.; Wisniewski, E. S.; Castleman, A. W. *Chem. Phys. Lett.* **2000**, *318*, 637.
(30) Mente, S.; Marconelli, M. *J. Phys. Chem. A* **1998**, *102*, 3860.
(31) Fernandez-Ramos, A.; Smedarchina, Z.; Siebrand, W.; Zgierski, M. *J. Phys. Chem.* **2001**, *14*, 7518.
(32) Herbich, J.; Hung, C. Y.; Thummel, R.; Waluk, J. *J. Am. Chem. Soc.* **1996**, *118*, 3508.
(33) Fiebig, T.; Chachisvilis, M.; Manger, M.; Zewail, A.; Douhal, A.; Garcia-Ochoa, I.; de La Hoz Ayuso, A. *J. Phys. Chem. A* **1999**, *103*, 7419.
(34) Taylor, C. A.; El-Bayoumi, M. A.; Kasha, M. *Proc. Natl. Acad. Sci. U.S.A.* **1969**, *63*, 253.
(35) Chang, C.; Shabestary, N.; El-Bayoumi, M. A. *Chem. Phys. Lett.* **1980**, *75*, 107.
(36) Sepiol, J.; Wild, U. P. *Chem. Phys. Lett.* **1982**, *93*, 204.
(37) Szemik-Hojniak, A.; Głowiak, T.; Deperasińska, I.; Puszko, A.; Talik, Z. *J. Nonlinear Opt. Quantum Opt.* **2003**, *30*, 215.
(38) *Xcalibur PX Software-CrysAlis CCD and CrysAlis-RED*, version 1.171; Oxford Diffraction Poland: Wrocław, Poland, 1995−2003.
(39) Sheldrick, G. M. *SHELXTL*, version 5.1; Bruker AXS: Madison, WI, 1998.
(40) O'Connor, D. V.; Phillips, D. *Time Correlated Single Photon Counting*; Academic Press: New York, 1984.
(41) Demas, J. N. *Excited State Lifetime Measurements*; Academic Press: New York, 1983.
(42) Frisch, M. J.; et al. *Gaussian 98*, revision A.9; Gaussian, Inc.: Pittsburgh, PA, 1998.
(43) *Quantum Chemistry Program Exchange*; Indiana University, Bloomington, IN, 1990; No. 455.
(44) Dewar, M. J. S.; Zoebish, E. G.; Healy, E. F.; Stewart, J. P. *J. Am. Chem. Soc.* **1985**, *107*, 3902.
(45) Böttcher, C. F. J. In *Theory of Electric Polarization*; van Belle, O. C., Bordewijk, P., Rip, A., Eds.; Elsevier: Amsterdam, 1973; Vol. 1.
(46) Mataga, N.; Kubota, T. *Molecular Interactions and Electronic Spectra*; Marcel Dekker: New York, 1970; pp 371−409.
(47) Szemik-Hojniak, A.; Głowiak, T.; Deperasińska, I.; Puszko, A. *J. Mol. Struct.* **2001**, *597*, 279.
(48) Szemik-Hojniak, A.; Głowiak, T.; Deperasińska, I.; Puszko, A. *Can. J. Chem.* **2002**, *80*, 1242.
(49) Rozas, I.; Alkorta, I.; Elguero, J. *J. Phys. Chem. A.* **1998**, *102*, 9925.
(50) Mordzinski, A.; Lipkowski, J.; Orzanowska, G.; Tauer, E. *Chem. Phys.* **1990**, *140*, 167.
(51) Woessner, G.; Goeller, G.; Kollat, P.; Stezowski, J. J.; Hausner, M.; Klein, U. K. A.; Kramer, H. E. A. *J. Phys. Chem.* **1984**, *88*, 5544.
(52) Schmidtke, S. J.; MacManus-Spencer, L. A.; Klappa, J. J.; Mobley, T. A.; McNeil, K.; Blank, D. A. *Phys. Chem. Chem. Phys.* **2004**, *6*, 1938.
(53) Hamilton, W. C.; Ibers, I. A. In *Hydrogen bonding in solids*; W. A. Benjamin: New York, 1968; p 116.
(54) Poór, B.; Michniewicz, N.; Kállay, M.; Buma, W. J.; Kubinyi, M.; Szemik-Hojniak, A.; Deperasińska, I.; Puszko, A.; Zhang, H. *J. Phys. Chem. A* **2006**, *110*, 7086.
(55) Zilberg, S.; Haas, Y. *J. Phys. Chem. A* **2002**, *106*, 1.
(56) Belau, L.; Haas, Y.; Rettig, W. *Chem. Phys. Lett.* **2002**, *364*, 157.
(57) Beens, H.; Weller, A. In *Organic Molecular Photophysics*; Birks, J., Ed.; Wiley: London, 1976; p 159.
(58) Deperasińska, I.; Dresner, J. *J. Mol. Struct.: THEOCHEM* **1998**, *422*, 205.